



Contents lists available at ScienceDirect

Image and Vision Computing

journal homepage: www.elsevier.com/locate/imavis

Zero-sum game theory model for segmenting skin regions

Djamila Dahmani*, Mehdi Cheref, Slimane Larabi

Computer Science Department, University of Science and Technology Houari Boumediene (USTHB), Algiers, Algeria

ARTICLE INFO

Article history:

Received 9 May 2019

Received in revised form 15 December 2019

Accepted 15 April 2020

Available online 30 April 2020

Keywords:

Skin detection

Color

Texture

Zero-sum game

Nash Equilibrium

ABSTRACT

This paper presents a new method for skin region segmentation based on a zero-sum game theory model which exploits the opposite classifications of an image region by different skin detectors. In fact, these regions are considered conflict areas between two players (skin and non-skin) and skin detectors are considered strategies. An appropriate utility function is then defined. The computation of the saddle point (The Nash equilibrium) in the mixed extension of the proposed zero-sum game allows classifying effectively the conflict areas and so reducing the false positive skin detection. Experiments were conducted on three publically available databases using four selected skin detectors based on skin color information, skin-texture cues and employ rule-based or neural networks. The results show that the proposed method outperforms the existing skin segmentation approaches in reducing the false positive rates and obtains promising results in the skin segmentation performance.

© 2020 Elsevier B.V. All rights reserved.

1. Introduction

Skin detection is still a challenging issue in image processing. It aims to determine whether a given video sequence, an image, a region or a pixel presents human skin [1]. Skin region segmentation determines the boundaries of skin regions such as hands and faces based on skin features such as color and texture. It has a huge number of computer vision applications such as face detection [2], hand gestures recognition [3,4], human computer-interaction [5], objectionable content filtering and video blocking [6,7], skin lesions segmentation [8,9] and image coding using region of interest [10,11].

Skin detection is a challenging task, due to the high variance of skin appearance in the image. These variations depend on some important factors such as: different ethnic groups, variations of illumination of skin areas in the same skin region, and skin-like color of backgrounds, and camera characteristics. Kawulok et al. established in [1] that using color alone may not improve the performance of the state-of-the-art for skin detection. This is principally due to the overlap between the skin and non-skin pixels in color spaces used.

There are numerous skin segmentation approaches proposed in the literature: rule-based methods, machine learning and Hybrid based methods. To detect skin pixels, most of these approaches use color [12,13] or texture features [14,15], or both of them [16]. The skin detection color-based methods are limited due to the

presence of objects in backgrounds having skin color, poor illumination condition, which produces detection of false positive errors in the segmentation result. Despite the aforementioned limitations, the color is still the most important feature to detect skin regions. Additional features such as texture may improve the stability of the color-based skin models by rejecting the regions which are not smooth [1]. Texture features consider that a sharp textural discrimination exists between skin and non-skin regions, in case of high and intermediate resolution of images.

By going through all the algorithms and skin classifiers developed in the literature, we can observe that all proposed methods can be efficient in some cases and not in other ones, it appears judicious to take advantage from each skin detector. In this perspective, we propose a novel skin segmentation method based on a zero-sum game theory model, which improves the detection efficiency and even surpasses the limits of some usual skin descriptors. The proposed method exploits the regions classified differently by a set of classifiers to improve the skin pixel detection. These regions can be viewed as conflict areas between skin and non-skin. They translate also the limitations or the weakness of the used skin classifiers. In these conflict areas, a zero-sum-game is established. The value of the game or the payoff of the optimum strategy is exploited to attribute the conflict region to the skin class or non-skin one. To implement the proposed game theoretic model, some classifiers were employed, namely the rule-based and Artificial Neural Networks (ANN) using both color and texture features.

The rest of the paper is organized as follows: Section 2 summarizes the related works in skin detection. The proposed method is explained in Section 3. Experimental evaluation is presented in Section 4 and finally our conclusions are reported in Section 5.

* Corresponding author.

E-mail addresses: ddahmani@usthb.dz (D. Dahmani), mehdi.cheref@etu.usthb.dz (M. Cheref), slarabi@usthb.dz (S. Larabi).

2. Related works

Numerous skin detection approaches have been proposed in the literature. The rule-based methods of skin detection are the earliest proposed methods. They were based on color cues such as thresholding-based techniques applied on various color spaces such as RGB [17], HSV [18] and YCbCr [19] explored using an elliptical skin color model, or on a combination of different color spaces [20]. More recently, the authors in [21] proposed an efficient skin pixel segmentation algorithm based on the correlation rules between the YCb and YCr subspaces. The correlation rules depend on the shape and size of skin color clusters determined dynamically. These clusters are computed for each single image and represent the areas containing most of candidates of skin pixels.

Model based techniques were also explored such as Bayesian classifier [12,21], Gaussian mixture [23], Artificial Neural Networks [24,25], and support vector machines [26]. Jones and Rehg introduced a Bayesian skin modeling based on the determination of skin probability for each color value [12]. They demonstrated that given a large amount of training data, even simple learning rules can yield good performance. Zhang et al. proposed a method based on adaptive thresholds and multi-layers perceptron to adjust the skin pixels detection [25]. The method presented in [22] was improved in [27] by including an Artificial Neural Networks classifier (ANN) to estimate an optimal acceptance threshold.

Approaches that included textural features to improve the skin color based segmentation were proposed [28,29]. In [28] textural features such contrast and homogeneity obtained from gray-level co-occurrence matrix (GLCM) were added to improve the YcbCr and RGB color based skin segmentation. The method can separate skin and non-skin color under complex background and has higher detection rate. The authors in [29], proposed a combination of a color based segmentation with texture analyzing. The texture features were extracted using 2-D Daubechies wavelets and represented as list of Shannon entropy. At first the Gaussian mixture model (GMM) classifier is applied for initial skin segmentation in RGB color space. Then the 2-D Daubechies wavelets are computed around each pixel classified skin pixel, to improve the skin detection. The non-skin regions were eliminated by the skin texture cluster elimination using k-mean clustering. In [30] an algorithm including color, texture and space information was proposed. At first the skin probability (SPM) in RGB color space was used. Then a filter utilizing the textural features extracted using Gabor wavelets is proposed to reduce the false acceptance rate. The authors in [31], improved the skin region classification by incorporating simple textural feature and stated that despite the fact that the textural cues have a low discriminating performance, they are able to improve stability of the color-based techniques. To increase the reliability of the skin detection process, neighborhood pixel information is incorporated into their proposed algorithm.

Recent approaches [16,32,33] used spatial analysis in skin segmentation and propagate the "skinness" starting with highly probable skin seeds. Kawulok introduced in [32] a distance for propoagating the Skinness from the seeds across the image in a combined domain of Luminance, hue and skin probability. The "skinness" propagating is performed using the shortest routes of the Dijkstra's algorithm. This method has important advantages to determine the region boundaries even in case of smooth transitions between the skin and non-skin pixels, and for its high stability. The method proposed in [33] has a considerable effectiveness in the skin detection. The authors explored how to exploit the textural cues to improve the propagation domain for skin spatial analysis. The textural features were extracted from the skin probability maps using a conventional Bayesian classifier developed in [12]. The textural cues thus determined have higher discriminative power than those extracted from the luminance channel. Then, they introduced the discriminative skin-presence features (DSPFs), which were used as domain for propagating the "skinness" This method was improved in [16] by incorporating self-adaptive seeds during the skin segmentation

process. The adaptive seeds were extracted using the skin probability map obtained from the input color image, and so did not require any skin sample for the adaptation process. The main advantage of the method is in providing the adaptiveness without making the method dependent on any other information sources.

Game theory is becoming nowadays, a robust mathematical tool in computer vision tasks, especially in image segmentation, classification and restoration. Kallel et al. proposed noisy image restoration and segmentation algorithm based on the computation of the pure Nash equilibrium [34]. Wang et al. developed image segmentation model using the game theory based optimization strategy [35]. In [36], Zhao et al. proposed Spectral-spatial classification scheme of hyperspectral imagery using cooperative game.

Differently from the existing methods, where multiple skin detection schemes are applied in additional manner to improve the skin region segmentation results, the approach proposed in this paper exploits the disagreement of skin detectors in the classification (skin or non-skin) of a region to classify it effectively. This disagreement is modeled by a zero-sum game where the skin and non-skin are defined as players. The strategies for the skin player are the classifiers that label the region as belonging to the skin, and the rest are the strategies for the non-skin player. The utility function is then defined based on a correlation distance. This distance uses visual features to quantify the dissimilarity of the region to skin. The utility function employs this distance on the region in consideration and its neighbors to allow for the homogeneity criteria. In addition, the computation of the correlation distance using skin sample obtained from the input image permits the system to be self-adaptive. The sign value in the mixed extension of the proposed zero-sum game is finally used to classify the region. The experiments show that considering the non-skin player as a decision agent allows reducing significantly the false positive rate detection when compared to the alternative approaches. Furthermore, an important underlining is that the proposed scheme can be applied with any number of classifiers and to any other binary classification conflict problems.

Our main contributions can be summarized as follows:

- Introduction of a new combination scheme for skin region segmentation that exploits the conflict regions i.e. regions classified differently by a set of skin detectors, to improve accuracy of the skin pixel detection.
- Proposition of an efficient zero-sum game theory model where the skin and non-skin regions represent the players.
- Development of a utility function which reduces the rate of the false positives (backgrounds pixels classified as skin pixels).

3. Proposed method

From a classification point of view, skin detection can be viewed as a two-class problem: skin-pixel vs. non-skin pixel classification [37]. The juxtaposition of the detection results of the existing skin pixel approaches especially those based on skin-color information or texture cues, will clearly show up many opposite pixel classifications or conflict areas.

We propose in this paper to model the skin pixel detection conflict problem as an evolutionary game. The main idea, on which this game rested, is to consider the conflict area as a disputed territory between two principal players (skin player and non-skin player). Each player would like to conquer all the identical territories to its nature and will face its own defeat if it penetrates the opposite territory. This game would perfectly fit into a zero-sum game (one player's loss is equal to the other player's gain), such as the pure strategies of each player are defined as being the different skin (non-skin) detectors used.

The saddle point in the mixed extension of this game will represent a compromise agreement between the two players, where the territory will be granted to the most persuasive player, according to the mixed value of the game. The purpose of this modeling in the skin-segmentation point of

view would be to reduce the false positive errors. In this section, we will first explain the proposed theoretic zero-sum game formulation, and the corresponding utility function. Then, in order to implement the theoretical concept presented in this paper, multiple skin classifiers (rule based and machine learning) are outlined to be employed as strategies in the proposed game.

3.1. The zero-sum game structure

We note S a set of skin classifiers. The image to be segmented is at first split into tiny regions or patches. If all classifiers of the set S agreed on certain patch it is classified appropriately, otherwise it is considered as a conflict patch. So, we note conflict patch or region as any region classified differently by at least one skin classifier belonging to the set S . In order to classify appropriately the conflict patches, a zero-sum game, is established to characterize the interaction between the two players in the conflict regions of the image.

The mathematical formulation of the problem can be presented as follows:

The proposed zero-sum game ϕ is defined by the given elements $\phi = (J, S_i, u)$, where:

- $J = \{skin\ player, non - skin\ player\}$.
- $S_i (i = 1, 2)$, the sets of pure strategies for each player in a conflict patch (region) P . S_i is subset of $S (S_i \subset S)$. The strategies sets $S_i, i = 1, 2$ are determined according to the conflict patch P :

$S_1 = \{s_i \in S : s_i\ classified\ P\ skin\}$ and $S_2 = \bar{S}_1$ the complement set of S_1 in S .

The strategies of the skin player are the classifiers belonging to the set S labeling the conflict Patch P as skin and the rest of the classifiers are the strategies of the non-skin player.

- u represents the utility function, it will be explained in the section below.

3.1.1. Utility or payoff function u and interactions

The payoff function is the main subject of this research effort, how can we define an appropriate payoff function providing a meaningful result?

Researches in human visual perception consider that the perceptual grouping is essentially based on the homogeneity and similarity criteria

[38,39]. The payoff function was based on these two aspects of visual perception. First, we have defined a skin-correlation distance that simulates the visual skin similarity aspect to recognize if the conflict region looks like a skin portion. The skin-correlation distance was then applied to the neighbors of the conflict region in order to verify the homogeneity of the area.

At the end the conflict patch will be considered as skin only if it verifies both visual skin similarity aspect and homogeneity norms. In the following we will introduce some relevant definitions and notations used to define the payoff function.

a. The correlation distance $d_{s_i, p}$

To define a distance between skin and no skin regions, we use a statistical approach based on the hypothesis that in the same image under the same lighting conditions the skin pixel features are usually similar. Because of the considerable amount of the no-skin data in the same image, only the skin data were considered in order to cope with different environments. More precisely for a conflict area P , the skin data used are all the regions in the same image that were classified skin by all classifiers $s_i \in S$.

The computation of this distance is always related to a specific strategy, the following steps show how to calculate a skin-correlation-distance of P related to a strategy s_i :

step 1. For each strategy $s_i \in S$, we define a skin data matrix M_{s_i} , each line of M_{s_i} represents skin features vector of s_i computed from a patch classified as skin by all the strategies $s_i \in S$ (for example the features vector of the strategy RGB, are the skin channels components R, G and B).

We note \bar{X}_j and σ_j the average and the standard deviation of the j^{th} variable in the skin data matrix M_{s_i} , given by the equations:

$$\bar{X}_j = \frac{1}{m} \sum_{i=1}^n X_{ij}; \sigma_j = \left(\frac{1}{m} \sum_{j=1}^n (X_{ij} - \bar{X}_j)^2 \right)^{\frac{1}{2}} \tag{1}$$

Where m is the number of skin patches and n the dimension of the features vector used in the strategy s_i .

The center of gravity of the matrix M_{s_i} is given by

$$G_{s_i} = (\bar{X}_1, \bar{X}_2, \dots, \bar{X}_n) \tag{2}$$

The standard deviation of the matrix M_{s_i} is given b

$$\sigma_{s_i} = (\sigma_1, \sigma_2, \dots, \sigma_n) \tag{3}$$

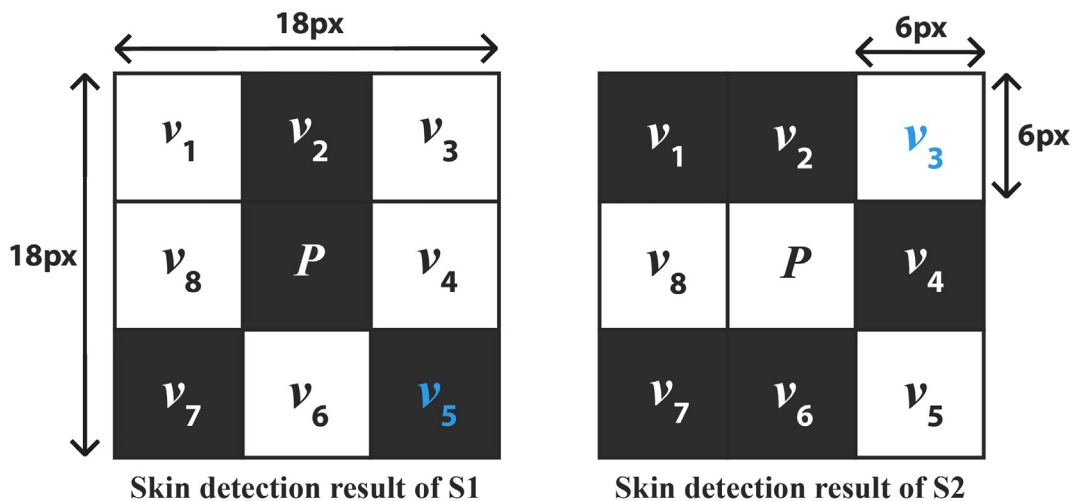


Fig. 1. Payoff calculation example.

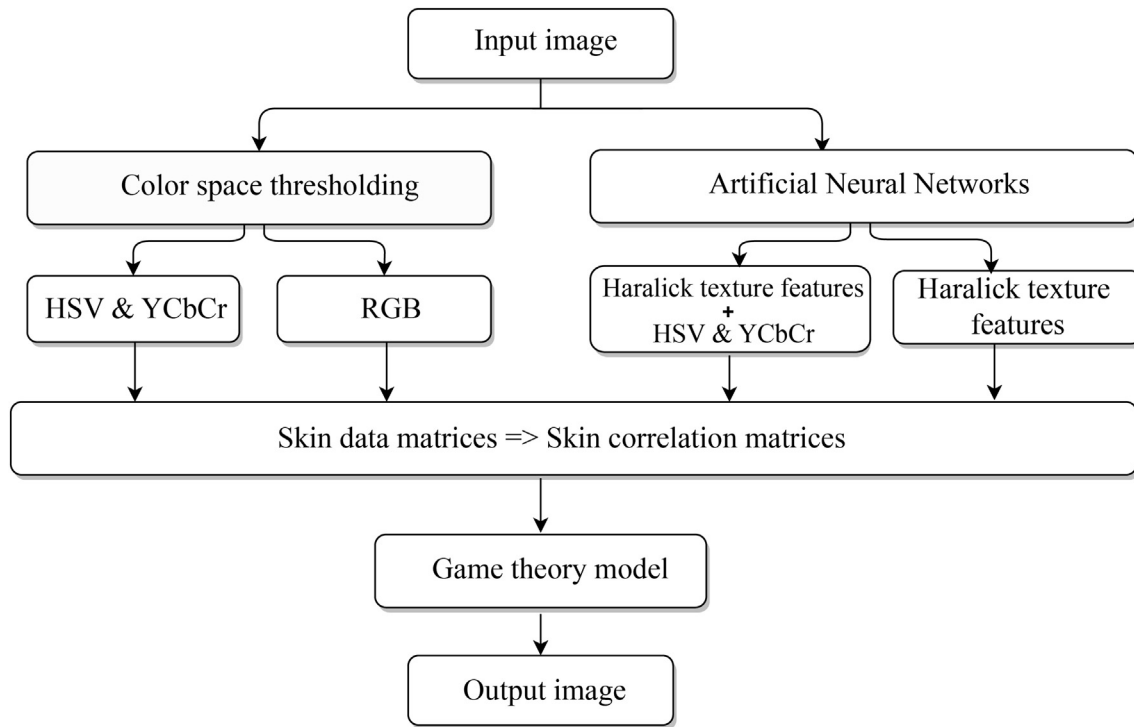


Fig. 2. Flowchart of the proposed method.

step 2. The centered and standardized matrix $Z_{s_i, p}$ obtained from the matrix M_{s_i} is computed by the following formula (4)

$$Z_{s_i} = \left(\frac{X_{11} - \bar{X}_1}{\sigma_1} \quad \dots \quad \frac{X_{1n} - \bar{X}_n}{\sigma_n} \quad \dots \quad \frac{X_{1m} - \bar{X}_1}{\sigma_1} \quad \dots \quad \frac{X_{mn} - \bar{X}_n}{\sigma_n} \right) \quad (4)$$

step 3. The correlation matrix R_{s_i} is computed using the eq. (5)

$$R_{s_i} = \frac{1}{m} Z_{s_i}^t Z_{s_i} \quad (5)$$

We note T_{s_i} the features vector of P associated with the strategy s_i

$$T_{s_i} = \begin{pmatrix} T_{s_i}^1 \\ \vdots \\ T_{s_i}^n \end{pmatrix} \quad (6)$$

Let \tilde{T}_{s_i} be the centered and standardized vector of T_{s_i} according to the data matrix M_{s_i} as shown in the formula (7)

$$\tilde{T}_{s_i} = \begin{pmatrix} \frac{T_{s_i}^1 - \bar{X}_1}{\sigma_1} \\ \vdots \\ \frac{T_{s_i}^n - \bar{X}_n}{\sigma_n} \end{pmatrix} \quad (7)$$

step 4. Let $Y_{s_i}^*$ be the vector belonging to the matrix Z_{s_i} such that $Y_{s_i}^* \in$

$\arg \min_{Y_{s_i} \in Z_{s_i}} \|\tilde{T}_{s_i} - Y_{s_i}\|$, where $\|\cdot\|$ represent the Euclidian distance.

step 5. Finally, we define the vector V_{s_i} such that $V_{s_i} = \tilde{T}_{s_i} - Y_{s_i}^*$,

The correlation distance $d_{s_i, p}$ which characterizes the similarity between the features vector of the patch P and the skin individuals data matrix M_{s_i} is then determined by the relation

$$d_{s_i, p} = V_{s_i}^t \times R_{s_i} \times V_{s_i} \quad (8)$$

The value of $d_{s_i, p}$ will be close to zero as long as the T_{s_i} is similar or close to the characteristic vectors of the data matrix M_{s_i} , this means that P is similar or approaching the image skin's characteristics. Otherwise the value of $d_{s_i, p}$ will be strongly greater than zero, this means that P is not similar and very different from the characteristic vectors of the data matrix M_{s_i} , in this case the closer to zero the entity $\frac{1}{d_{s_i, p}}$ would be, the farther the computed features are from the skin characterization.

Since the skin similarity aspect had been modeled, the utility function will explore this perspective to ensure the homogeneity norms.

b. Utility function formula.

If s_1 is the first player's strategy "Skin" and s_2 the strategy of the second player "non-skin", the intuition behind the computation of the utility function $u(s_1, s_2)$ is to compare the similarity of the patch P to skin pixels in the image according to s_1 classification, with its dissimilarity according to s_2 classification. This comparison allows determining which of the two classifiers (strategies) is more accurate in its classification, and so translating the fact that one player has overcome the second using an interactive formula at the pair (s_1, s_2) .

Table 1
Details of ANN architectures.

| ANN Database | ANN Texture-color | | | ANN Texture |
|--------------------|-------------------|--------|--------|-------------|
| | HGR1 & HGR2A | HGR2B | SFA | All |
| Hidden layer | 3 | 9 | 3 | 10 |
| Neurons | 9 | 11 | 11 | 14 |
| Score on test data | 94.75% | 94.85% | 97.62% | 86.5% |

Table 2
Game-theory model evaluation as combination scheme compared to the selected classifiers.

| Databases | Classifiers | SP | F-measure | G-measure | D_{prs} |
|------------|------------------------|----------------|----------------|----------------|----------------|
| HGR | RGB | 0.85632 | 0.47929 | 0.50086 | 0.72187 |
| | HSV-YCbCr | 0.97687 | 0.79393 | 0.79407 | 0.29269 |
| | Texture-ANN | 0.9207 | 0.61774 | 0.62504 | 0.54321 |
| | Texture-Color-ANN | 0.9854 | 0.86729 | 0.86739 | 0.18884 |
| | Game-theory(GTH) model | 0.9938 | 0.8854 | 0.88712 | 0.17567 |
| Pratheepan | RGB | 0.73763 | 0.55759 | 0.60015 | 0.65853 |
| | HSV-YCbCr | 0.82517 | 0.60537 | 0.62509 | 0.57767 |
| | Texture-ANN | 0.77721 | 0.55732 | 0.58633 | 0.6455 |
| | Texture-Color-ANN | 0.79809 | 0.55734 | 0.57972 | 0.64112 |
| | Game-theory(GTH) model | 0.82152 | 0.63322 | 0.62389 | 0.58118 |
| SFA | RGB | 0.98143 | 0.83265 | 0.83807 | 0.26014 |
| | HSV-YCbCr | 0.96901 | 0.85447 | 0.85601 | 0.21645 |
| | Texture-ANN | 0.98094 | 0.82709 | 0.83286 | 0.26804 |
| | Texture-Color-ANN | 0.95079 | 0.87097 | 0.87096 | 0.189 |
| | Game-theory(GTH) model | 0.96948 | 0.87969 | 0.88035 | 0.17768 |

The bold data represent the best result rate of a metric (Specificity ,Recall F-measure, G-measure, Dprs or δ_{fp}).

For that we need at first to quantify the similarity of the patch P to the skin pixels according to the strategy (classifier) s_1 , and the dissimilarity of P to skin pixels of the image according to the strategy (classifier) s_2 . These quantifications are based on the distance defined in the previous formula 8, and the notion of similarity of the skin or non-skin in the neighborhood of P (homogeneity norms).

If we note V the set of the skin neighbors' patches of P according to the strategy s_1 , we define α the similarity of P to skin neighbors' pixels by the eq. (9)

$$\alpha = \min_{v \in V} |d_{s_1,P} - d_{s_1,v}| \sum_{v \in V} d_{s_1,v} \tag{9}$$

Where $d_{s_1,v}$ represents the distance defined by the formula (8).

α is the product of two factors. The first one allows estimating the similarity of the patch P to its skin pixels neighbors. It is determined by computing the minimum value obtained when comparing the correlation distance of P to the correlation distances of its skin neighbors according to the classifier s_1 . The second part quantifies the similarity of all the skin neighbors of P to skin according to the classifier s_1 . It represents a homogeneity index. α will be closer to zero when the characteristics of P and its neighbors are significantly close to the characteristics of the skin pixels of the image.

With the same manner, we can define the entity β which quantifies the similarity distance of P to the non-skin pixels (the dissimilarity to skin) according to the strategy (skin-classifier) s_2 . We use the inverse distance computed from the skin data matrix M_{s_2} as explained in the Section 3.1.1. (a).

$$\beta = \min_{v \in \bar{V}} \left| \frac{1}{d_{s_2,P}} - \frac{1}{d_{s_2,v}} \right| \sum_{v \in \bar{V}} \frac{1}{d_{s_2,v}} \tag{10}$$

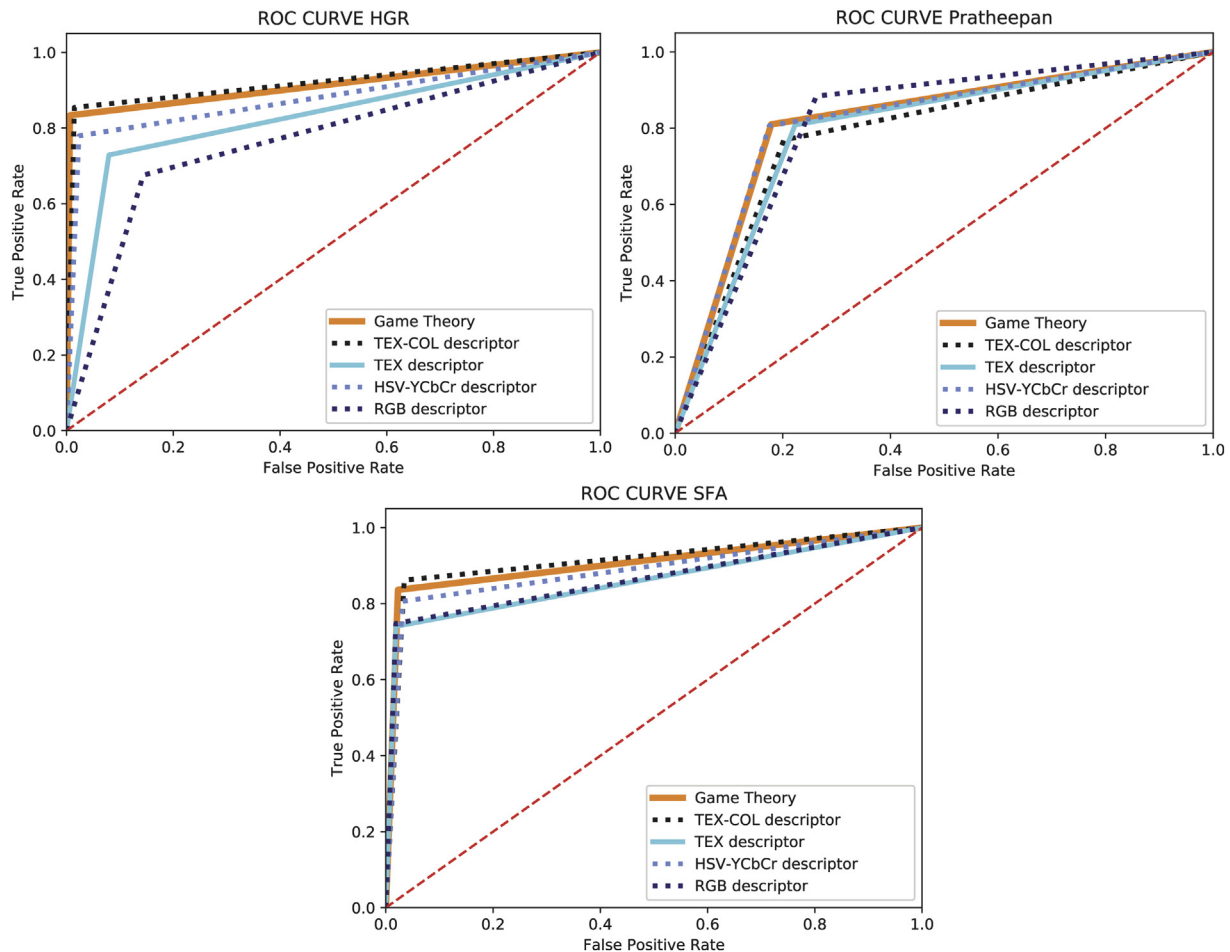


Fig. 3. Classifiers Comparison using the ROC Curves in the three databases.

Where \bar{V} represent the set of non-skin neighbors of P according to the classification of the strategy s_2 .

With the same reasoning as for the entity α , the entity β will be closer to zero when the characteristics of P and its neighbors according to the classifier s_2 are significantly far from the characteristics of the skin pixels of the image.

Then we define the payoff function $u(s_1, s_2)$ as being the difference between α and β . It can be given by the formula (11)

$$u(s_1, s_2) = \beta - \alpha = \min_{v \in \bar{V}} \left| \frac{1}{d_{s_2, P}} - \frac{1}{d_{s_2, v}} \right| \sum_{v \in \bar{V}} \frac{1}{d_{s_2, v}} - \min_{v \in \bar{V}} |d_{s_1, P} - d_{s_1, v}| \left| \sum_{v \in \bar{V}} d_{s_1, v} \right| \quad (11)$$

So, the sign of the real $u(s_1, s_2)$ is positive if the patch P is closer to the skin and negative otherwise. This fact translates the zero-sum game

interaction between the skin and non-skin players. Fig. 1 presents an example of the payoff function calculation, where:

- v_i in black/white are the neighbors of P classified as skin/non-skin by the classifiers s_1, s_2 respectively.
- v_5 and v_3 represent the neighbors of P such that:

$$\min_{v \in \bar{V}} |d_{s_1, P} - d_{s_1, v}| = |d_{s_1, P} - d_{s_1, v_5}| \text{ and } \min_{v \in \bar{V}} \left| \frac{1}{d_{s_2, P}} - \frac{1}{d_{s_2, v}} \right| = \left| \frac{1}{d_{s_2, P}} - \frac{1}{d_{s_2, v_3}} \right|$$

Therefore, the calculation of $u(s_1, s_2)$ will be as follows

$$u(s_1, s_2) = \left| \frac{1}{d_{s_2, P}} - \frac{1}{d_{s_2, v_3}} \right| \left(\frac{1}{d_{s_2, v_3}} + \frac{1}{d_{s_2, v_5}} + \frac{1}{d_{s_2, v_8}} \right) - |d_{s_1, P} - d_{s_1, v_5}| \left(d_{s_1, v_2} + d_{s_1, v_5} + d_{s_1, v_7} \right)$$

| | Original image | RGB | HSV-YCbCr | Texture | Texture-color | GTH model | Mask |
|-----|----------------|-----|-----------|---------|---------------|-----------|------|
| (1) | | | | | | | |
| (2) | | | | | | | |
| (3) | | | | | | | |
| (4) | | | | | | | |
| (5) | | | | | | | |
| (6) | | | | | | | |
| (7) | | | | | | | |
| (8) | | | | | | | |

Fig. 4. Game theory (GTH) model performance against selected classifiers in HGR database.

3.1.2. Saddle point or Nash Equilibrium in the zero-sum game

After the elaboration of the game matrix A in a conflict patch, the computing of the saddle point or the Nash Equilibrium, will allow to

settle the conflict, so in segmentation terms to attribute the conflict patch to the skin player or the no-skin one. The value of a zero-sum game is the payoff value of the optimal strategies for each player.

| | Original image | RGB | HSV-YCbCr | Texture | Texture-color | GTH model | Mask |
|---------------------------|----------------|-----|-----------|---------|---------------|-----------|------|
| SFA DATASET | | | | | | | |
| img (37) | | | | | | | |
| img (42) | | | | | | | |
| img (586) | | | | | | | |
| img (102) | | | | | | | |
| Pratheepan DATASET | | | | | | | |
| YuFamilyPhoto | | | | | | | |
| obama | | | | | | | |
| Megan-Fox | | | | | | | |
| Matthew_narrowweb | | | | | | | |

Fig. 5. Game theory model performance in SFA and Pratheepan databases.

| | (a) | (b) | (c) | (d) | (e) | (f) | (g) |
|----------------|-----|-----|-----|-----|-----|-----|-----|
| Original image | | | | | | | |
| Mask | | | | | | | |
| Our methode | | | | | | | |
| (1) | | | | | | | |
| (2) | | | | | | | |
| (3) | | | | | | | |
| (4) | | | | | | | |
| (5) | | | | | | | |
| (6) | | | | | | | |
| (7) | | | | | | | |

Table 3
Quantitative evaluation of the proposed method.

| measurements | methods | Image Databases | | |
|---------------|----------------------------|-----------------|----------------|----------------|
| | | HGR | Pratheepan | SFA |
| F-measure | Jones end Rehg [12] | 0.83341 | 0.68831 | 0.79987 |
| | Kovac et al. [17] | 0.70153 | 0.62625 | 0.79852 |
| | Cheddad et al. [51] | 0.78352 | 0.59523 | 0.55032 |
| | Chen et al. [52] | 0.71930 | 0.60281 | 0.78810 |
| | Kawulok [32] | 0.84496 | 0.71941 | 0.85551 |
| | Kawulok et al. [33] | 0.89486 | 0.65494 | 0.83440 |
| | Kawulok et al. [16] | 0.70372 | 0.69188 | 0.87343 |
| | Proposed method | 0.89633 | 0.76171 | 0.89123 |
| Recall | Jones end Rehg [12] | 0.96173 | 0.89123 | 0.76255 |
| | Kovac et al. [17] | 0.83839 | 0.90944 | 0.79658 |
| | Cheddad et al. [51] | 0.96278 | 0.93632 | 0.64793 |
| | Chen et al. [52] | 0.93988 | 0.93523 | 0.83856 |
| | Kawulok [32] | 0.97757 | 0.89451 | 0.90696 |
| | Kawulok et al. [33] | 0.97507 | 0.92759 | 0.88283 |
| | Kawulok et al. [16] | 0.99021 | 0.94638 | 0.94648 |
| | Proposed method | 0.85180 | 0.77944 | 0.85003 |
| G-measure | Jones end Rehg [12] | 0.84092 | 0.71305 | 0.80082 |
| | Kovac et al. [17] | 0.71107 | 0.65900 | 0.79851 |
| | Cheddad et al. [51] | 0.79745 | 0.64466 | 0.55667 |
| | Chen et al. [52] | 0.73996 | 0.64492 | 0.78952 |
| | Kawulok [32] | 0.85071 | 0.73360 | 0.85688 |
| | Kawulok et al. [33] | 0.89881 | 0.68520 | 0.83565 |
| | Kawulok et al. [16] | 0.75516 | 0.71834 | 0.87604 |
| | Proposed method | 0.89755 | 0.76190 | 0.89207 |
| Specificity | Jones end Rehg [12] | 0.93944 | 0.83450 | 0.94172 |
| | Kovac et al. [17] | 0.90349 | 0.78762 | 0.91971 |
| | Cheddad et al. [51] | 0.91345 | 0.72667 | 0.71421 |
| | Chen et al. [52] | 0.88221 | 0.75076 | 0.88294 |
| | Kawulok [32] | 0.94117 | 0.87358 | 0.91374 |
| | Kawulok et al. [33] | 0.96428 | 0.80682 | 0.90569 |
| | Kawulok et al. [16] | 0.85587 | 0.83152 | 0.91072 |
| | Proposed method | 0.99145 | 0.94289 | 0.97674 |
| D_{prs} | Jones end Rehg [12] | 0.27422 | 0.43104 | 0.29162 |
| | Kovac et al. [17] | 0.43927 | 0.57119 | 0.29603 |
| | Cheddad et al. [51] | 0.35229 | 0.63296 | 0.69124 |
| | Chen et al. [52] | 0.43786 | 0.61206 | 0.32499 |
| | Kawulok [32] | 0.26359 | 0.43104 | 0.22880 |
| | Kawulok et al. [33] | 0.17853 | 0.53519 | 0.25747 |
| | Kawulok et al. [16] | 0.47660 | 0.48790 | 0.21589 |
| | Proposed method | 0.15803 | 0.34210 | 0.16445 |
| δ_{fp} | Jones end Rehg [12] | 6.05555 | 16.5495 | 5.82797 |
| | Kovac et al. [17] | 9.65065 | 21.2371 | 8.02882 |
| | Cheddad et al. [51] | 8.65452 | 27.3322 | 28.5785 |
| | Chen et al. [52] | 11.7786 | 24.9233 | 11.7054 |
| | Kawulok [32] | 5.88237 | 12.6419 | 8.62550 |
| | Kawulok et al. [33] | 3.57137 | 19.3170 | 9.43090 |
| | Kawulok et al. [16] | 4.47137 | 16.8473 | 8.92732 |
| | Proposed method | 0.85421 | 5.70169 | 2.32574 |

The bold data represent the best result rate of a metric (Specificity, Recall, F-measure, G-measure, D_{prs} or δ_{fp}).

Therefore, the fairest manner to assign a conflict patch to skin or non-skin class is to focus only on the sign value of the game. If this value is equal to zero the game is fair, if it is positive, the game favors the skin player, while if it is negative; we say the game favors the no-skin player.

The value doesn't always exist in pure games, so we use the mixed (randomized) extension of the game ϕ noted $\bar{\phi}$ and described by the given elements $\bar{\phi} = (J, \Delta(S_i), \mu)$ where $\Delta(S_i)$ is the set of all probability distributions over S_i .

$$\Delta(S_i) = \left\{ x \in \mathbb{R}^{|S_i|} : x_i \geq 0 \text{ and } \sum_1^{|S_i|} x_i = 1 \right\} \text{ for } i = 1, 2 \quad (12)$$

$\mu = E(u(x, y))$ is obtained from the payoff function u of the eq. (11) in the zero-sum pure game and the mathematical expectation of the profile (x, y) such that $(x, y) \in \Delta(S_1) \times \Delta(S_2)$.

According to the notations above:

$$\mu = E(u(x, y)) = x^t A y \quad (13)$$

Where A is the payoff matrix of the game determined in previous Section 3.1.1(b).

In his fundamental Minimax Theorem (the Main Theorem of the theory of Games) Von Neumann [40] established the existence of a unique value v^* in mixed finite games such that:

$$\max_{x \in \Delta(S_1)} \min_{y \in \Delta(S_2)} x^t A y = \min_{y \in \Delta(S_2)} \max_{x \in \Delta(S_1)} x^t A y = v^* \quad (14)$$

And some optimal mixed strategies x^*, y^* (Nash equilibrium profile (x^*, y^*)) such that the expected payoff v^* is calculated by eq. (15).

$$(x^*)^t A y^* = v^* \quad (15)$$

Thus v^* is the maximum "floor" of the Player 1 and minimum "ceiling" of player 2.

A solution (x^*, y^*, v^*) of the game matrix A can be obtained by the resolution of linear optimization problem as follows:

For the player 1 the linear problem (LP) is:

$$v^* = \max v \quad (16)$$

$$\sum_{i \in S_1} x_i a_{ij} \geq v \quad \forall j \in S_2 \quad (17)$$

$$\sum_{i \in S_1} x_i = 1 \quad x_i \geq 0 \quad \forall i \in S_1 \quad (18)$$

Similarly for the player 2 the dual linear problem (linear complementary problem) CLP is:

$$u^* = \min u \quad (19)$$

$$\sum_{j \in S_2} y_j a_{ij} \leq u \quad \forall i \in S_1 \quad (20)$$

$$\sum_{j \in S_2} y_j = 1 \quad y_j \geq 0 \quad \forall j \in S_2 \quad (21)$$

It was proven that there is a polynomial time algorithm for finding a mixed Nash equilibrium in a two-player zero-sum game [41].

In this paper, we use the sign of value v^* (the expected payoff) in a conflict patch to classify the patch in skin (first player) or no-skin (second player) class. If v^* is equal to zero ($v^*=0$) the patch is attributed to skin class.

To illustrate the theoretical concept of the proposed game theory model, we select four usual skin pixel detection methods in classification pattern:

Fig. 6. Skin detection results (a), (b), (c) and (d) from HGR database, (e) from Pratheepan database and (f) and (g) from SFA database. (1) Kawulok et al., [16], (2) Kawulok et al., [33], (3) Kawulok [32], (4) Chen et al., [52], (5) Cheddad et al., [51];(6) Kovac et al., [17], and (7) Jones and Rehg [12].

- Two skin classifiers based on an explicit color space thresholding.
- Two skin classifiers based on Artificial Neural Networks (ANN), the first explores only the skin texture features and the second explores both skin color and texture features.

These methods will constitute afterward, the set of strategies in the proposed conflict game. Fig. 2 summarizes the steps of the proposed method.

3.1.3. Rule-based strategies (color space thresholding)

In most cases, the skin may be seen as a portion of the image having a specific color. Using the boundaries of this area as the threshold for an image, it is possible to extract the pixels whose color can be likened to that of the skin. The explicit skin color thresholding is one of the easiest and usually used approaches. In this paper, the proposed system operates on 3 different color spaces the RGB, HSV, and YCbCr.

a. RGB color space (RGB thresholding strategy).

In the RGB space, the model proposed by [42] is used. This shows that the color of the skin pixel level must meet the following rules:

$$(R > 97) \wedge (G > 40) \wedge (B > 20) \wedge (\max(R, G, B) - \min(R, G, B)) > 15 \wedge (R - G) > 15 \wedge (R > G > B) \quad (22)$$

b. HSV and YCbCr color spaces (HSV-YCbCr thresholding strategy).

The HSV color space can be obtained from the RGB space using a non-linear transformation and constitutes a very good choice for skin detection methods [37]. Besides, the orthogonal color spaces reduce the redundancy present in RGB color channels. Among the orthogonal color spaces the YCbCr space is one of the most used color space in the skin detection. In this paper, we propose to use the complementary information provided by the two color spaces by regrouping them within thresholding conditions for skin pixel detection.

Only channels Cb, Cr and H, S are selected by the application of the threshold, because Y and V represent intensity (luminance) information. The skin cluster is described in the two color spaces by the rules:

$$0 \leq H \leq 50 \wedge 0.23 \leq S \leq 0.68 \wedge 85 \leq Cb \leq 135 \wedge 135 \leq Cr \leq 180 \quad (23)$$

3.1.4. Artificial neural networks (ANN based strategies)

Differently from the rule-based methods, the skin model can be learned from training sets of skin and no-skin pixels using machine learning approaches. Artificial Neural Networks (ANN) were used in the literature for individual skin pixel classification based on its color values. In this paper we explore firstly the texture values of skin pixels to train an Artificial Neural Networks classifier, and then the texture and color values of skin pixels are used to train another ANN classifier.

a. Texture Strategy (Texture-ANN).

The skin texture alone was not largely used for skin pixel detection, but it was even so proved that the skin texture attributes can ameliorate the skin detection operation. In this paper we use the spatiotemporal aspect of the skin texture based on Gabor filter [43] along with the statistical one by computing the Haralick indices [44] from the filtered image.

The texture analyses process in this paper come along the following steps:

Algorithm 1. Texture analysis process.

Texture analysis process

- 1: **function** TEXTANALYSIS(IRGB) IRGB is an RGB 6x6 pixel area from the input image
- 2: IHSV \leftarrow Convert IRGB to HSV color space
- 3: IHSVGBr \leftarrow Apply Gabor filter to IHSV
- 4: IHSVGBrTogray \leftarrow Convert IHSVGBr to gray level scale
- 5: GLCM \leftarrow compute gray level co-occurrence matrix from IHSVGBrTogray
- 6: HaralickFeatures \leftarrow compute 13 Haralick features from the GLCM
- 7: **return** HaralickFeatures
- 8: **end function**

The Gabor filters used in this paper are from different orientations from 0 to π , with a step of $\frac{\pi}{6}$. The 13 indices are extracted from average matrix of the co-occurrences matrices (GLCM) computed with distance $d = 1$ and four different orientations $0, \frac{\pi}{2}, \pi, \text{ and } \frac{2\pi}{6}$. Finally the characteristics vector composed by the 13 Haralick indices is used to train Artificial Neural Network classifier (ANN) for skin pixel detection. More details are given in the Experimental results section.

b. Color-Texture Strategy (Color-Texture-ANN).

In this last description the color attributes are mixed along with the texture ones. We used the Hue and Saturation components H, S from the HSV color space, the blue and red chrominance components Cb and Cr from the YCbCr color space, and the 13 Haralick indices extracted from the Gabor filtered images defined in (a). These color and texture features taken on independent channels are used to train an Artificial Neural Network (ANN). The ANN's architecture providing the best classification score is not the same for the three databases used in the experimental phase. More details about these architectures are given in the [Experimental results](#) section.

3.2. Skin pixel detection process

The [algorithm 2](#) given below describes the proposed skin detection process. For each conflict area we integrate a zero-sum game model in order to find an agreement. In a particular case where only one classifier disagrees with the others, the optimum strategy can be inferred directly.

In this case $|S_i| \leq 3$, so the computation of the value complexity is very low, but there is a big number of game matrices which corresponds to the number of conflict patches in the image. To solve this problem, the image was divided into sub-images and the skin classification was performed in a parallel architecture.

Algorithm 2. Skin pixel detection.

Skin pixel detection

- 1: **procedure** SKINDETECTION(UIImage)
- 2: ConflictArea \leftarrow array()
- 3: size \leftarrow 0
- 4: **for** each 6x6 pixel area "P" from UIImage **do**
- 5: CharacteristicVectors \leftarrow array()
- 6: P-HSV \leftarrow Convert P to HSV color space
- 7: P-YCbCr \leftarrow Convert P to YCbCr color space
- 8: CharacteristicVectors["RGB"] \leftarrow mean RGB values of P
- 9: CharacteristicVectors["HS-CbCr"] \leftarrow mean HS-CbCr values from both P-HSV and P-YCbCr
- 10: CharacteristicVectors["Texture"] \leftarrow **Texture analyses process** (P)
- 11: CharacteristicVectors["Texture-color"] \leftarrow CharacteristicVectors["Texture"] + CharacteristicVectors["HS-CbCr"]
- 12: **Get-Detection-Result-From-each-classifier** (CharacteristicVectors)

```

13:     if the four classifiers classify P as skin then
14:         P is classified definitely as skin
15:         Add each vector from the CharacteristicVectors to its specific
           skin data matrix
16:     else
17:         if the four classifiers classify the region as non-skin then
18:             P is classified definitely as non-skin
19:         else
20:             ConflictArea[j] ← CharacteristicVectors
21:             size ← size + 1
22:         end if
23:     end if
24: end for
25: for each CA in ConflictArea do
26:     Apply the zero-sum-game model to CA
27: end for
28: end procedure

```

4. Experimental results

The experiments of the proposed method were conducted using three datasets: Hand Gesture Recognition database HGR (HGR1, HGR 2A, HGR 2B) [45], human skin detection dataset Pratheepan [46], and face detection database SFA based on two classical face detection databases namely AR face database [47] and FERET face database [48].

4.1. Conducted tests and obtained results

During the first experiments, we studied the proposed game theory model's performance in improving the combination of the selected classifiers. Details of used ANN architectures for each database are given by Table 1.

Table 2 represents the quantitative evaluation when testing the proposed game theory model on some images from the three databases. The measurements used in this step are Specificity (SP), F-measure [49], G-measure and D_{prs} [50]. If we note TP the number of skin pixels correctly classified as skin pixels, TN the number of no-skin pixels correctly classified as no-skin pixels, FP the number of no-skin pixels classified skin pixels and FN the number of skin-pixels classified no-skin pixels. The above measurements are given by the formulas:

$$PR = \frac{TP}{TP + FP} \quad (24)$$

$$RE = \frac{TP}{TP + FN} \quad (25)$$

$$SP = \frac{TN}{TN + FP} \quad (26)$$

$$F\text{-measure} = \frac{2PR \times RE}{PR + RE} \quad (27)$$

$$G\text{-measure} = \sqrt{PR \times RE} \quad (28)$$

$$D_{prs} = \sqrt{(1-PR)^2 + (1-RE)^2 + (1-SP)^2} \quad (29)$$

For HGR database, the proposed game theory model improved the results obtained by each classifier for the four metrics selected. In the SFA database, three metrics among the four selected were improved.

Three metrics in Pratheepan database were not improved according to only the HSV-YCbCr classification but the performance differences in all cases are very small of order 10^{-3} . It is interesting to underline that the selected metrics highlight different aspects of the skin detection methods. Seldom, a combination method improves all aspects of combined classifiers. These results demonstrate the performance of the game theory model proposed as a combination scheme.

Another way to show the quantitative performance of the game theory model compared to the selected classifiers is by plotting the ROC (receiver operating characteristic) curves. The ROC curves of each classifier and of the proposed game theory model computed from the three databases are presented in Fig. 3. We remark that for SFA database the game theory model outperforms the selected classifiers. Moreover, in Pratheepan database, our model kept the highest score achieved by the HSV-YCbCr classifier and slightly below the highest score recorded by the Texture-color Skin classifier in HGR database. The Pratheepan dataset images are captured with a range of different cameras using different color enhancements, so the use of skin texture cues for classification may bring confusion and so not improving the skin detection process. We have to say also that the game theory model has always recorded the smallest false positive rate in the three databases.

The qualitative performance can be shown in Fig. 4 for HGR database. The examples in HGR database were selected from the HGR1, HGR2A, and HGR 2B. It is evident that the proposed game theory model provided better accuracy than each classifier in segmenting skin pixels in the given sample images. We can notice also that the conflict areas, namely the areas classified differently by the selected skin pixel classifiers were attributed to their true class by the game theory model classifier. Furthermore, we can remark that the background pixels misclassified as skin pixels (false positive) by the selected classifiers were eliminated using the proposed game theory model. The proposed zero-sum game model is particularly suited to the classification of the conflict in which the classifiers provide opposite decision.

Likewise experimental results of the game theory model compared to the selected classifiers as combination scheme in SFA and Pratheepan databases are presented in Fig. 5. In both databases, the game theory model provided better accuracy in segmenting skin pixels and particularly decreased the number of background pixels misclassified as skin pixels by the selected classifiers. These experimental results proved the effectiveness of the game theory model to reduce the false positive errors provided by the classifiers, and so it can be efficient as a combination method.

4.2. Comparative evaluation

In this section we will present the qualitative and quantitative comparative results of the proposed approach when applied to the three databases. Our algorithm has been compared with the most cited works among the literature (Jones and Rehg [12]; Kovac et al., [17]; Cheddad et al., [51]; Chen et al., [52]; Kawulok [32]; Kawulok et al. [33] and Kawulok et al., [16]. Some results of the methods for the HGR, Pratheepan and SFA databasae are reported in Fig. 6.

By observing Fig. 6, it is obvious that the proposed method provides better accuracy in segmenting skin pixels in the given sample images than the seven existing techniques. In all series of HGR database, the game theory model reduces and usually eliminates the background pixels classified as skin pixels (false positives) by the other techniques. The algorithms in [12,16,32,33] are based on the determination of initial skin seeds, which are then used to propagate the skin regions. These seeds are detected using color channels. Erroneous skin seeds in background propagate false skin regions, which results in high false positive rate. Differently from these approaches, the opposite classification given by the classifiers in a conflict region is exploited in our method to classify it correctly. This is carried out by establishing a zero-sum interaction in the conflict area. The computation of the mixed Nash equilibrium allows detecting the correct class and removing the tenacious discord. The proposed modeling has permitted to reduce enormously the false positive regions as we can observe it in the sample images of the Fig. 6.

Table 3 presents a quantitative comparison with all the algorithms reported in this section. For HGR database and differently from the related works where only HGR 1 is used for the computation of the metrics, images from the three datasets namely HGR1, HGR 2A and HGR 2B were used in this paper. There are multitude of metrics for performance evaluation of skin segmentation algorithms. Different measures can give different values considered as optimal by one condition, but not by another. For more general comparison, the selected metrics in this paper are: F-measure, Recall, G-measure, Specificity, D_{prs} , and false positive rate δ_{fp} .

Table 3 shows that the proposed method tested on the three databases outperforms, overall the other methods in terms of five measures among the six considered, namely F-measure, specificity, D_{prs} , and false positive rate δ_{fp} , except for HGR database in G-measure, when our algorithm achieved the second best score with a small difference about 0.001. G-measure can only increase when the precision and recall are high; it reflects the general classification of algorithms. Specificity indicates the capability of a classifier to recognize patterns of a negative class to determine real negative situations correctly labeled as negative [53]. The specificity of the proposed method is very interesting it is about 0.99145 when computed from HGR database; this is due to the ability of the proposed utility function to reduce the non-skin regions detected as conflict areas. D_{prs} metric can be considered as 3D generalization of 2D ROC, and takes into account the recall, precision and specificity measures. In the proposed algorithm D_{prs} achieved independently from the chosen database the best result with an average score about 2%, 9% and 5% better than the second classified method. The false positive rate δ_{fp} of the proposed method is about 0.85421 in HGR database. This result asserts that the proposed method has an important efficiency in the reduction of the false positive rate.

Finally the Recall of the proposed method is lower than the other methods. This aspect is generally due to the reduction of the false positives, at the expense of the true positives. In the proposed classification scheme, a region is considered as conflict region if at least one classifiers; $\in S$ disagrees with the others about its classification. This reasoning led to a strict decision that significantly reduced the rate of the false positives but this induced also that some skin regions were classified as non-skin due to a poor lighting or an important variance of the skin appearance in the same image, thus reducing the recall factor.

5. Conclusion

In this paper we proposed a new skin segmentation method based on zero-sum game theory model. There are three major contributions in this work. The first one is the introduction of new combination scheme, which can be extended to different skin detection classifiers. The proposed scheme exploits the weakness of skin detectors to improve the skin region segmentation. The obtained results showed the effectiveness of this combination scheme to take the best of each classifier. The second one a zero-sum game theory model for skin detection is proposed. In this game the skin and non-skin regions represent players. This new vision of skin detection task allows reducing significantly the non-skin regions detected as skin ones, particularly in the presence of skin like color backgrounds. The third contribution is the proposed utility function that appears to be efficient in binary classification conflict problems.

The experiments conducted on three publically available databases and using six skin detection performance metrics, show that our method provides promising results in terms of qualitative and quantitative evaluations. When taking into account five metrics about the six selected, the proposed algorithm was best ranked, compared with seven state-of-art works, widely cited in the literature.

CRedit authorship contribution statement

Djamila Dahmani: Conceptualization, Methodology, Formal analysis, Writing - original draft, Writing - review & editing, Validation, Investigation. **Mehdi Cheref:** Conceptualization, Software, Writing - original draft, Writing - review & editing, Investigation. **Slimane Larabi:** Supervision, Visualization, Writing - review & editing.

References

- [1] M. Kawulok, J. Nalepa, J. Kawulok, Skin Detection and Segmentation in Color Images, *Advances in Low-Level Color Image Processing*. Springer, 2014 (pp. 329-366).
- [2] Z. Zakaria, S.A. Suandi, J.M. Saleh, Hierarchical Skin-AdaBoost-Neural Network (H-SKANN) for multi-face detection, *Applied Soft Computing*, 68, 2018, pp. 172-190.
- [3] S. Bilal, R. Akmeiliawati, Salami MJE, A.A. Shafie, Dynamic approach for real-time skin detection, *J Real-Time Image Process*, 10, 2012, pp. 371-385.
- [4] M. Kawulok, Dynamic skin detection in color images for sign language recognition, *Proceedings of the ICISP, LNCS*, vol 5099, Springer 2008, pp. 112-119.
- [5] Y. Zhu, G. Xu, D.J. Kriegman, A real-time approach to the spotting, representation, and recognition of hand gestures for human-computer interaction, *Comput. Vision Image Understand*, 85 (3), 2002, pp. 189-208.
- [6] J. Stöttinger, A. Hanbury, C. Liensberger, R. Khan, Skin Paths for Contextual Flaggging Adult Videos, *Advances in Visual Computing*. Springer, 2009 (pp. 303-314).
- [7] L. Daxiang, Z. Xiaoqiang, L. Ying, Pornographic images filtering using pmkbased mil algorithm, *Int. J. Comput. Sci.* 10 (3) (2013).
- [8] T.Y. Tan, L. Zhang, S.C. Neoh, C.P. Lim, Intelligent skin cancer detection using enhanced particle swarm optimization, *Knowledge-Based Systems*, 158, 2018, pp. 118-135.
- [9] A. Baldi, R. Murace, E. Dragonetti, M. Manganaro, S. Bizzi, Automated contentbased image retrieval: application on dermoscopic images of pigmented skin lesions, *Skin Cancer*. Springer 2014, pp. 523-528.
- [10] M.-J. Chen, M.-C. Chi, C.-T. Hsu, J.-W. Chen, Roi video coding based on h. 263 + with robust skin-color detection technique, *IEEE Trans. Consumer Electron.* 49 (3) (2003) 724-730.
- [11] S.-F. Huang, M.-J. Chen, M.-S. Li, Region-of-interest segmentation based on bayesian theorem for h. 264 video transcoding, *IEEE Visual Communications and Image Processing (VCIP)*, IEEE 2011, pp. 1-4.
- [12] M.J. Jones, J.M. Rehg, Statistical color models with application to skin detection, in: *Int. J. Comput. Vision* 46 (1) (2002) 81-96.
- [13] N. Brancati, G.D. Pietro, M. Frucci, L. Gallo, Human skin detection through correlation rules between the YCb and YCr subspaces based on dynamic color clustering, *Computer Vision and Image Understanding* 2017, pp. 155:33-42.
- [14] P. Ng, C.-M. Pun, Skin Color Segmentation by Texture Feature Extraction and Kmean Clustering, in: *Third International Conference on Computational Intelligence, IEEE, Communication Systems and Networks (CICSyN)*, 2011 (pp. 213-218).
- [15] C. Dumitrescu, I. Dumitrache, Human skin detection using texture information and vector processing techniques by neural networks, in: L. Dumitrache (Ed.), *Advances in Intelligent Control Systems and Computer Science*, Vol. 187 of *Advances in Intelligent Systems and Computing*, Springer, Berlin Heidelberg 2013, pp. 59-75.
- [16] M. Kawulok, J. Kawulok, J. Nalepa, B. Smolka, Self-adaptive algorithm for segmenting skin regions, *EURASIP J. Adv. SignalProcessing* 170 (2014) 1-22, <https://doi.org/10.1186/1687-6180-2014-170>.

- [17] J. Kovac, P. Peer, F. Solina, Human skin color clustering for face detection, in: EUROCON computer as a tool 2 (2003) 144–148.
- [18] K. Sobottka, I. Pitas, Face localization and facial feature extraction based on shape and color information, In: Proceedings of the IEEE international conference on image processing (ICIP) 3 (1996) 483–486.
- [19] R.L. Hsu, M. Abdel-Mottaleb, A. Jain, Face detection in color images, IEEE Trans Pattern Anal Mach Intell, 24(5), 2002, pp. 696–706.
- [20] G. Kukharev, A. Nowosielski, Fast and efficient algorithm for face detection, in colour images, Mach. Graphics Vis. 1230–0535 (13) (2004) 377–399.
- [21] N. Brancati, G.D. Pietro, M. Frucci, L. Gallo, Human skin detection through correlation rules between the YCb and YCr subspaces based on dynamic color clustering, Computer Vision and Image Understanding, 2017, (pp.155:33–42).
- [22] S. Phung, A. Bouzerdoum, D. Chai, Skin segmentation using color pixel classification: analysis and comparison, IEEE Trans Pattern Anal Mach Intell, 2005, (pp. 27(1): 148–154).
- [23] H. Reenspan, J. Oldberger, I. Eshet, Mixture model for face-color modeling and segmentation, Pattern Recogn Lett, 2001, pp. 22:1525–1536.
- [24] M.J. Seow, D. Valaparla, V. Asari, Neural network based skin color model for face detection, Proceedings of the Applied Imagery Pattern Recognition Workshop, 2003, (pp. 141–145).
- [25] M.-J. Zhang, W.-Q. Wang, Q.-F. Zheng, W. Gao, Skin-color detection based on adaptive thresholds. In: Proceedings of IEEE ICIG, ISBN 0-7695-2244-0, 2004, pp. 250–253.
- [26] M. Kawulok, J. Nalepa, Support vector machines training data selection using a genetic algorithm. In: Statistical techniques in pattern recognition, S+SSPR 2012, LNCS, vol 7626, Springer, 2012, pp 557–565.
- [27] J.-S. Lee, Y.-M. Kuo, P.-C. Chung, E.-L. Chen, Naked image detection based on adaptive and extensible skin color model. in: Pattern Recognit., 0031–3203 40, 2007, pp. 2261–2270.
- [28] X. Wang, X. Zhang, J. Yao, Skin Color Detection under Complex Background, Proceedings of IEEE MEC, In, 2011 (pp. 1985–1988).
- [29] P. Ng, C.M. Pun, Skin color segmentation by texture feature extraction and k-mean clustering. In: Proceedings of the 2011 3rd international conference on computational intelligence, communication systems and networks (CICSyN), 2011, pp. 213–218.
- [30] Z. Jiang, M. Yao, W. Jiang, Skin detection using color, texture and space information, in: proc, IEEE FSKD 3 (2007) 366–370.
- [31] A. Taqa, H. Jalab Increasing the reliability of skin detectors, in :Sci Res Essays 5(17), 2010, pp. 2480–2490.
- [32] M. Kawulok, Fast propagation-based skin regions segmentation in color images, in: 10th IEEE International Conference and Workshops on Automatic Face and Gesture Recognition (FG), IEEE, 2013, pp. 1–7.
- [33] M. Kawulok, J. Kawulok, J. Nalepa, Spatial-based skin detection using discriminative skin-presence features, in : Pattern Recogn. Lett. 41 (2014) 3–13.
- [34] M. Kallel, R. Aboulaichb, A. Habbal, M. Moakhere, A Nash-game approach to joint image restoration and segmentation. in: Applied Mathematical Modelling Volume 38, Issues 11–12, 1 June 2014, pp. 3038–3053.
- [35] T. Wang, Q. Sun, Z. Ji, Q. Chen, P. Fu, Multi-layer graph constraints for interactive image segmentation via game theory. in: Pattern Recognition 55, 2016, pp. 28–44.
- [36] J. Zhao, Y. Zhong, T. Jia, X. Wang, Y. Xu, H. Shu, L. Zhang, Spectral-spatial classification of hyperspectral imagery with cooperative game. in: ISPRS Journal of Photogrammetry and Remote Sensing 135, 2018, pp. 31–42.
- [37] P. Kakumanu, S. Makrogiannis, N. Bourbakis, A survey of skin-color modeling and detection methods. in: Pattern Recognition 40, 2007, pp. 1106–1122.
- [38] T. Feldmann-Wüstefeld, A. Schubö, Stimulus homogeneity enhances implicit learning: Evidence from contextual cueing, in: Vision Research (97), 2014, pp. 108–116.
- [39] B. Pinna, D. Porcheddu, K. Deiana, From Grouping to Coupling: A New Perceptual Organization in Vision, Psychology, and Biology, in: Front Psychol. 7(1051), 2016 pp. 1–23.
- [40] J. Von Neumann, Zur Theories der Gesellschaftsspiele, Math. Ann, 100, 1928, pp. 295–320.
- [41] N. Nisan, T. Roughgarden, E. Tardos, V.V. Vazirani “Algorithmic game theory”, in: Cambridge press, ISBN-13: 978-0521872829, 2007.
- [42] P. Peer, F. Solina, An automatic human face detection method, in: Univerza v Ljubljani, 1999, pp. 122–130.
- [43] J. P. Jones, & L. A. Palmer, An evaluation of the twodimensional gabor filter model of simple receptive fields in cat striate cortex, in: Journal of Neurophysiology, 58(6), 1987, pp. 1233–1258.
- [44] R. Haralick, K. Shanmugan, I. Dinstein, Textural features for image classification, In: IEEE Transactions On Systems, Man, and Cybernetics SMC-3 (1973) 610–621.
- [45] Database for Hand Gesture Recognition (HGR), 2013. <http://sun.aei.polsl.pl/mkawulok/gestures/>, (accessed 15-april-2018).
- [46] Human skin detection dataset, <http://cs-chan.com/downloadsskindataset.html>. (accessed 18-august-2018).
- [47] A. Martinez, R. Benavente, The AR Face Database, Purdue University, Technical report, 1998.
- [48] P. J. Phillips, H. Wechsler, J. Huang, and P. J. Rauss, The facial recognition technology (FERET) database, 1996, <https://www.nist.gov/programs-projects/face-recognition-technology-feret>. (accessed 10-june-2018).
- [49] R. Khan, A. Hanbury, J. Stöttinger, A. Bais, Color based skin classification, Pattern Recogn Lett 33 (2) (2012) 157–163.
- [50] K. Intawong, M. Scuturici, S. Miguet, A New Pixel-Based Quality Measure for Segmentation Algorithms Integrating Precision, Recall and Specificity, Computer Analysis of Images and Patterns. Springer, In, 2013 (pp. 188–195).
- [51] A. Cheddad, J. Condell, K. Curran, P.M. Kevitt, A skin tone detection algorithm for an adaptive approach to steganography. in: Signal Process 89 (12), 2009, pp. 2465–2478.
- [52] Y.H. Chen, K.T. Hu, S.J. Ruan, Statistical skin color detection method without color transformation for real-time surveillance systems. in: Engineering Applications of Artificial Intelligence, vol. 25, no. 7, 2012, pp. 1331–1337.
- [53] M. Qahtan Yas, A. A. Zadain, B. B. Zaidan, Bahbib Rahmatullah, H. Abdul Karim, Comprehensive insights into evaluation and benchmarking of real-time skin detectors: Review, open issues & challenges, and recommended solutions. in: Measurement 114, 2018, pp. 243–260.